Detectable Super-Continuum Group in Photonics rock Crystal Fibre

[1]Akhilesh Kumar Chauhan, [2]Shailesh Kumar Singh
[1]M.Sc. Student Monad University, Hapur
[2]Head and Professor Monad University Hapur

Abstract: Super-continuum spreading after 450-1200 nm with 0.74 W regular power was generated in PCF consuming frequency doubled up light on or after a double phase fiber amplifier. The ordinary Super-continuum influence was presented as linearly accessible with the pulse reverberation percentage whereas the extreme productivity power was partial by the core size of the gain Fibre, and existing pump power. Arithmetical replications established that the widest Super-continuum range essential pumping in the uncharacteristic scattering system neighboring to the PCF λ0. Additional augmentation of the continuum bandwidth is probable over a two-step Super-continuum generation method — MI prompted pulse disintegration in a tiny length of irregular spreading PCF surveyed by SPM lengthening in a perfect scattering less high non-linearity material.

Index Terms - Super-continuum, scattering system, PCF, MI, SPM

I. INTRODUCTION

Detectable Super-continuum group in Photonics rock-crystal fibers have remained broadly deliberate consuming a variety of pump sources. Advanced Super-continuum average power productivity in superfluous of a watt consume remained gained by pumping by mode protected picosecond pulses from an Yb Fibre laser at 1060 nm. Different methods have been established to cover the Super-continuum spectrum just before the blue. Super-continuum encompassing down to 400 nm was proved spending a microchip laser at 1064 nm to pump a PCF with revised generation guide in the infra-red to resourcefully stage equal with unfathomable blue wavelengths. Multi-wavelength pumping arrangements concerning a pump and it's another harmonic or four wave collaborating pump changes has also been confirmed to rise spectral exposure in the visible. The procedures declared beyond using mode locked lasers undergo commencing one main shortcoming — deficiency of average power scalability in arrears to static recurrence rate. The capability to fluctuate the pulse recurrence amount is intrinsic to several Super-continuum schemes consuming microchip lasers and main oscillator power amplifier category pumps. But, the Mechanism of the Super-continuum normal power by fluctuating the recurrence rate whereas protection the peak power perpetual has not been confirmed earlier. In this review a humble nanosecond foundation based on frequency copying amplified increase substituted pulses from a regular 1.55 μm telecom laser diode is confirmed as a robust substitute to mode-locked laser centered setups. The arrangement of a review is define minutiae of Investigational circumstance used to create the observable Super-continuum. The Investigational results show progression of the Super-continuum spectrum with topmost power and power scalability of the Super-continuum productivity. Arithmetical reproductions of the non-linear Schrödinger equation are accomplished to regulate the Super-continuum group apparatuses and appreciate the boundaries of the wavelength edge. Finally, a different process to outspread the small wavelength edge spending a two phase Super-continuum group method. The major phase practices MI to yield high ultimate power Femtosecond pulses whereas the succeeding phase uses a low distribution but high non-linearity material to accomplish large spectral augmentation through self-phase modulation.

EXPERIMENTAL SETUP

A block chart of the all fiber combined extraordinary power pump arrangement at 1.55 μm is illustrated in Fig. 1 1553 nm DFB laser diode is focused by a pulse generator to yield 2 ns pulses at adjustable recurrence rates and amplified consuming double stage fibre amplifiers. The major phase contains of a 1 m long 4/125 m Erbium doped fibre amplifier (EDFA) forward pumped by a 400 mW 980 nm single mode laser diode. In order to improve the noise performance of the system, the amplified natural emission (ASE) generated by the first stage amp is filtered using a 100 GHz band pass filter adjusted at the seed laser wavelength. An isolator between the two gain stages prevents loss to the constituents in the pre-amp from backward circulating light in the power-amp phase. The power-amp stage includes a 5m long 7/125 μm cladding pumped Erbium-Ytterbium co-doped fiber amplifier (EYFA) backward pumped by two 8W 976 nm multi-mode laser diodes fixed into the gain fibre via a 6+1:1 pump combiner. At the highest operating recurrence rate of 1 MHz, the power-amp created an output of 3.2W average power (1.6 kW peak power).

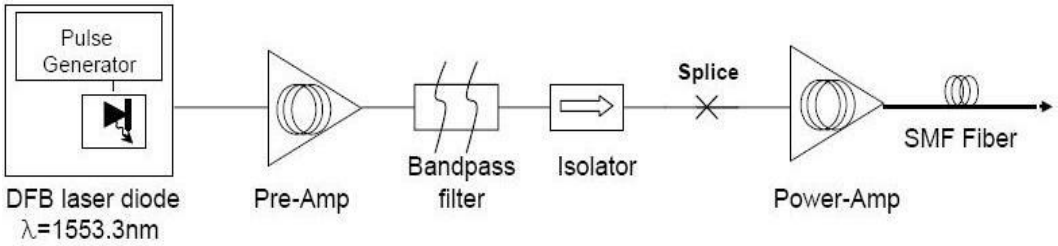

Fig.1. All fiber integrated high power 1553 nm pump system

The light at 1553 nm is then frequency doubled consuming an occasionally poled lithium niobate (PPLN) crystal already existence coupled into the PCF. The Investigational planning for the second harmonic generation process (SHG) followed by visible Super-continuum generation is shown in Fig. 2. A quarter wave plate and half-wave plate at the production of the power-amp are used to regulate the polarization state of the light. The light then passes through a free space optical isolator previously existence coupled into a 10 mm long PPLN crystal temperature relieved at 160C. The crystal temperature and the spot size of the intensive beam within the PPLN are optimized for exciting SHG Efficiency

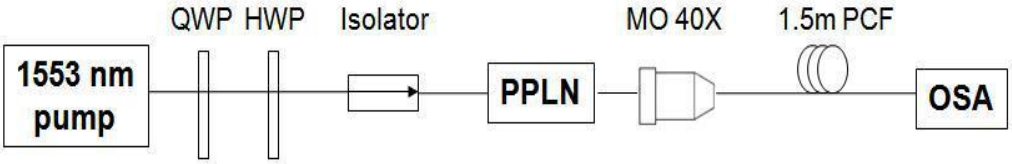

Fig. 2. Experimental setup for SHG and visible SC generation

Later the PPLN crystal consumes a narrow doubling bandwidth of ~1 nm, spectral broadening in the amplifier decreases the SHG efficacy. To decrease non-linearity, the distance of the SMF-28 production Fibre in the power-amp was reduced to ~0.5 m. Next, the input peak power was varied to obtain maximum SHG efficacy ~70% at 1 Kw (Fig. 2). The hypothetical efficacy for a lossless crystal at the given peak power is ~99%. But then again, the transmission loss over the crystal at low power was measured as ~30%, and thus the extreme conversion efficacy likely experimentally was reached. With an auxiliary growth in peak power, the efficacy starts to drop as the amplifier output spectrum broadens and more power shifts outside the 1 nm conversion bandwidth of the rock crystal.

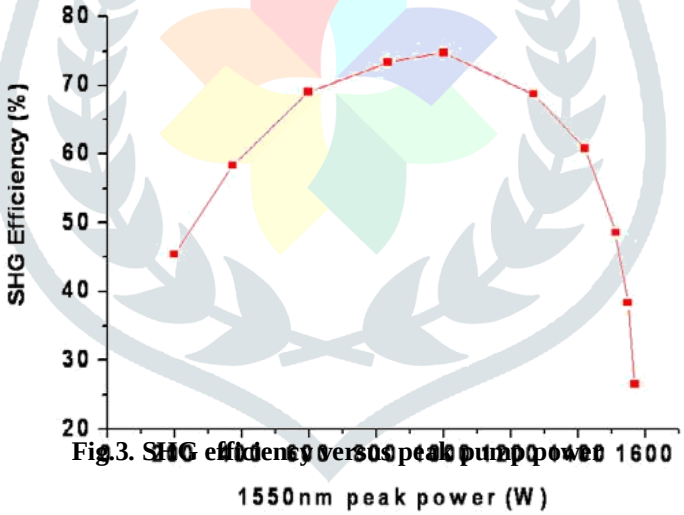

Fig.3. SHG efficiency versus peak pump power

The frequency gathered productivity on or after the PPLN at 776.5 nm deeds as the pump source for continuum generation in the PCF. The light is then coupled into a 1.5 m extended PCF (core diameter = 1.9 μm, λ0 = 745 nm, dispersal slope at λ0 = 0.85 ps.nm^{-2}km^{-1}) with ~50% link efficacy using a 40X microscope detached. The output spectrum is noted by means of an optical spectrum analyzer with a 2 nm resolve.

EXPERIMENTAL RESULTS

The production continuum from the PCF for a pump (776.5 nm) highest power of 420 W is shown in Fig.4. The continuum spreads from 450-1200 nm with 0.74 W time be around power. The spectrum is charming from 550-750 nm by superior than 2dB flat ness diagonally this wavelength range. Apart from the peak at the pump wavelength, some totaling crests can be pragmatic in the output spectrum. The peak at ~518 nm is owing to third harmonic generation from the PPLN, whereas the peak at ~388 nm ascends from stage matched four wave involvement. To standardize the perpendicular axis of the spectrum, the zone under the spectral arc was arithmetically computed and compared to the total SC power as resolute by a thermal power meter.

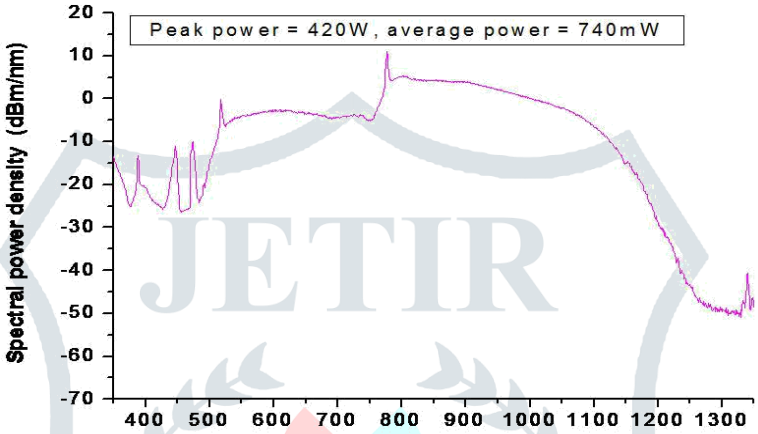

Fig.4. SC output spectrum from 1.5 m PCF for an input peak power of 420W

Resulting, the SC spectral progression as a task of input peak power was studied. Since the fiber is pumped with nanosecond pulses in the anomalous dispersion region, we expect the SC growth to be initiated by MI [8, 10]. In the time domain, this implies that the 2 ns pulse breaks up into a train of periodic Femtosecond solitons. As the peak power is increased to 110 W, the characteristic MI spectral side bands around the pump wavelength are observed. The asymmetry in the spectral power density of the short and long wavelength regions arises due to the different continuum generation mechanisms responsible for each side. The long wavelength side of the spectrum experiences additional gain due to stimulate Raman scattering which, transfers power from shorter to longer wavelengths. On the other hand, wavelengths below the pump is generated primarily by phase matched FWM [8, 11]. The smooth nature of the continuum can be attributed to the ensemble average of spectra produced by multiple solitons within the 2ns pulse envelope.

NUMERICAL REPLICATIONS

To determine the wavelength limits of the generated SC and identify the generation mechanisms, numerical simulations of the generalized non-linear Schrodinger equation were performed using the adaptive split-step Fourier method. The complex envelope *A* (*z, τ)* of a pulse, under the slowly varying approximation satisfies the generalized

$$\frac{\partial A}{\partial z} = (N+D)\,A$$

$$D = -\frac{i}{2}\beta_2 \frac{\partial^2 A}{\partial \tau^2} + \frac{1}{6}\beta_3 \frac{\partial^3 A}{\partial \tau^3} + \frac{i}{24}\beta_4 \frac{\partial^4 A}{\partial \tau^4} - \frac{\alpha}{2}$$

$$N = i\gamma\left(1 + \frac{i}{\omega_0}\frac{\partial}{\partial t}\right)$$

$$\int_{-\infty}^{+\infty} [(1 - f_R)\delta(t) + f_R\, h_R(t)]|A(z, t - t')|^2 dt'$$

Second ($\beta 2$), third ($\beta 3$) and the fourth order ($\beta 4$) dispersion as well as the loss (α) of the fiber. The terms in the operator $\hat{N}$ result from nonlinear interactions, which describe self-phase modulation, self-steepening and stimulated Raman scattering effects. In particular, the effective nonlinearity is defined as $\gamma = n_2 \omega_0 / c A_{eff}$, where *n2* and *A eff* are the nonlinear refractive index and effective mode area of the fiber respectively. In addition, *hR (t)* represents the Raman response function, and *fR* is the fractional contribution of the Raman response to the nonlinear polarization. To reduce computation time, a 20 ps super-Gaussian pulse at 776.5 nm was fed as the input to our simulator. Simulations with broader pulse widths (up to 200 ps) were also performed and showed no significant difference in the spectrum obtained.

Figure 5 shows comparison between experiment and simulation results for 1.5 m of PCF with γ = 65 $W^{-1}km^{-1}$. The pump wavelength is 776.5 nm and the peak power is 420 W. The differences between the 2 curves can be explained as follows. On the short wavelength side, the experimental spectrum shows additional peaks between 350-550 nm that are not present in the simulation. As mentioned earlier in section 2.3, the peak at 518 nm is due to third harmonic generation from the PPLN crystal, while that at 388 nm is due to four wave mixing between the 518 nm and 777 nm signals. The additional peaks at 440 nm and 475 nm are also attributed to the same phase matched process. Since the simulator only assumes a delta function input at the second harmonic frequency of 776.5 nm, and does not include the weak third harmonic at 518 nm, the various phase matched peaks due to the four wave mixing process are not present in the simulated spectrum. On the long wavelength side, simulation results show higher power than the experimentally obtained spectrum. While the simulator assumes a constant mode field diameter (MFD) across the entire wavelength range, the MFD actually increases for long wavelengths as the guiding properties of the fiber become weaker. Thus, the effective non-linearity at long wavelengths is smaller in the experiment compared to the simulations, resulting in a lower continuum level.

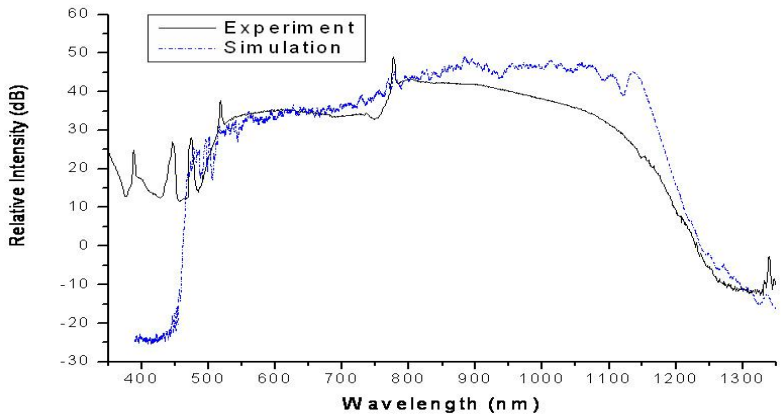

Fig. 5. Comparison of experimental and simulation spectra for 1.5m PCF at 420W peak power

To confirm that the SC generation is initiated by MI, simulations with fibers having different zero dispersion wavelengths but the same dispersion slope 0.85 $ps.nm^{-2}km^{-1}$ were performed. In each case, the common parameters were the pump wavelength λp = 776.5 nm, peak power P = 420 W and non-linear coefficient γ = 65 $W^{-1}km^{-1}$. Figure 6(a) shows the output spectrum after propagation through 0.3 m of fibers with $\lambda 0$ ranging from 745 nm to 775 nm. We observe symmetrical side bands around the pump wavelength and obtain maximum broadening for the fiber with $\lambda 0$=775 nm. This is consistent with

MI, since MI phase matches only when the pump is in the anomalous dispersion region and the gain bandwidth is inversely proportional to the separation of the pump wavelength from the fiber $\lambda 0$. The theoretical MI gain coefficient is given by,

$$g = \sqrt{(\gamma P)^2 - [\left(\Delta k/_2\right) + \gamma P}$$

$$\Delta k = -\frac{\lambda^2}{2\pi c} \left[\frac{dD}{d\lambda}|_{\lambda_0}\left(\lambda_p - \lambda_v\right)\right](\omega_p - \omega_s)^2$$

After propagation through a length L of the fiber, the power gain experienced by the L = 0.3 m for fibers with different λ0 and the results are in excellent agreement with figure 6.This confirms that modulation instability is the dominant non-linear effect in the initial propagation through the PCF. Initially, anomalous dispersion plays an important role in breaking up the quasi-CW pulse into ultra-short pulses required for SC generation. Thus, while MI seeds the SC generation process, MI alone cannot account for the final continuum bandwidth obtained. The resulting ultra-short pulses further broaden the spectrum as they propagate down the fiber through an interplay of self-phase modulation, stimulated Raman scattering and phase matched four wave mixing. But, as the continuum evolves towards the blue wavelength region, the large normal dispersion of the PCF prevents efficient four wave mixing. In other words, the short wavelength edge of the continuum is limited by phase mismatch caused by the fiber dispersion.

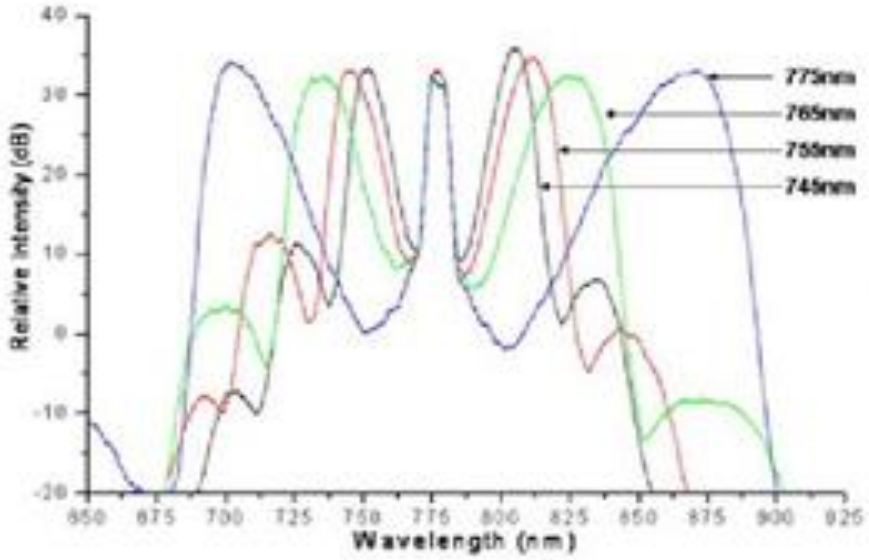

a

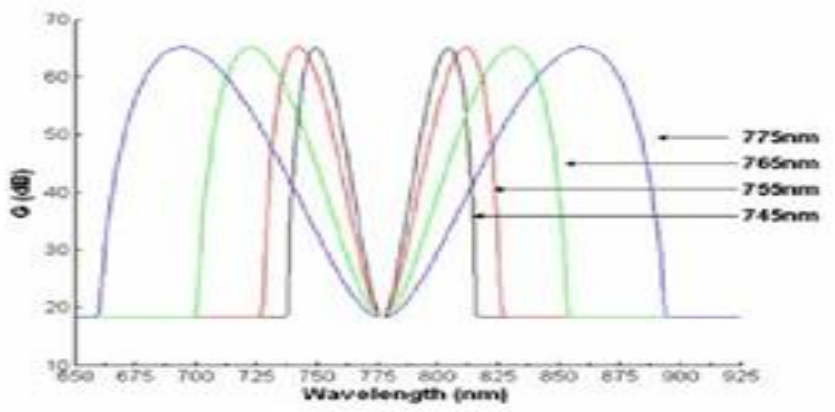

(b)

Figure-6 Output after 0.3m PCF for different λ_0 (a) Simulation output (b) Theoretical MI power gain.

DISCUSSION

In this segment, a 2 stage model based on separation of the pulse break-up and spectral broadening stage is proposed to optimize the short wavelength SC generation process. In the first stage, a short length of PCF is pumped in the anomalous dispersion regime to break-up the nanosecond pulse into a train of ultra-short femtosecond pulses through MI. In the second stage, a material with high Kerr non-linearity (large nonlinear refractive index n2) and minimal dispersion is used to maximize spectral broadening. Simulation results for the 2 stage model are presented below. Figure 2.9 shows the temporal output after propagating through 0.5 m of PCF with λ0 = 745 nm and λp = 776.5 nm. The initial 20 ps super-Gaussian pulse is broken up into ~20 fs wide pulses with ~3x the original intensity. The separation between pulses is ~74 fs and is in excellent agreement with the Theoretical separation given by

$$T = \frac{2\pi}{\sqrt{\frac{2\gamma P_0}{|\beta_2}}} = 73\ fs$$

Where P_0 = 420 W, γ = 65 $W^{-1}km^{-1}$ and β_2 = -7.39e-3 ps^2/m

The narrow pulses from the 1st stage PCF are then launched into an ideal 2nd stage dispersion less material with non-linearity comparable to the PCF. The output spectra for different lengths of the 2nd stage material are shown in Fig. 7. We observe symmetric and smooth broadening around the pump wavelength indicative of SPM as the primary broadening mechanism. On the other hand, Fig. 8 shows the results for the same propagation length in a single stage PCF. The corresponding spectra are asymmetric and much narrower as further spectral broadening is ultimately limited by fiber dispersion. The 20 dB SC bandwidth after just 4 cm of stage 2 material is ~425 nm compared to ~230 nm for the single stage, an enhancement of almost 2x.

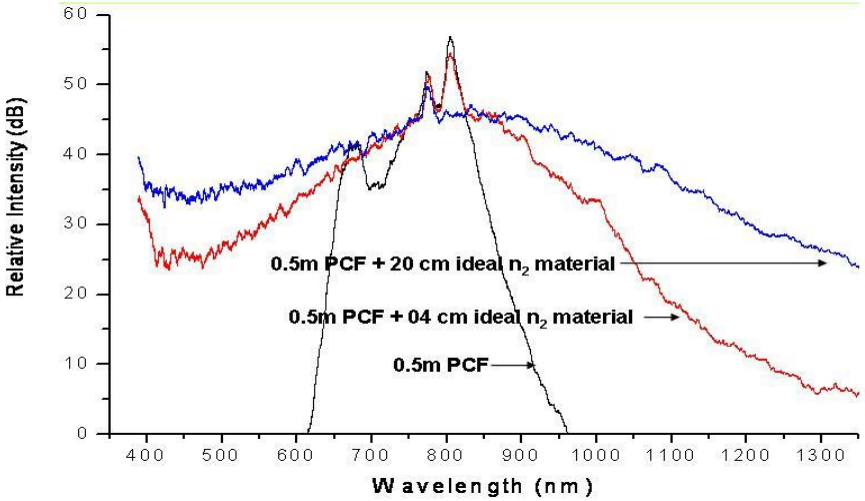

Fig. 7. Spectra from two stage model: 0.5m 745 nm λ_0 PCF followed by ideal n_2 material

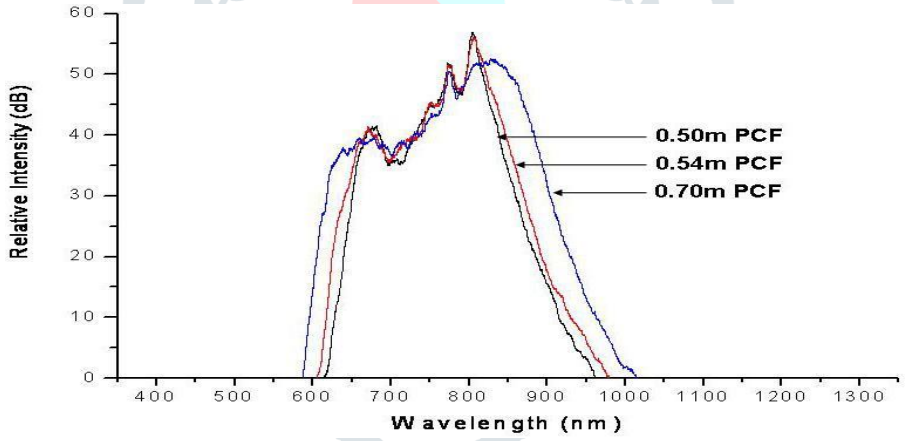

Fig. 8. Spectra from single stage model: 0.50-0.70m of 745 nm λ_0 PCF

The choice of the 2nd stage material is based on the relative values of the dispersion Length (L_D) and non-linear length (L_{NL}). The dispersion length is given by $L_D = \tau_{0/}^2 / |\beta_2$ and the nonlinear length is LNL 1/ (γ P) , where $\tau 0$ is the FWHM of the soliton from the 1st stage and P is the peak power. While it is essential for the 1st stage PCF to be pumped in the anomalous regime, the 2nd stage can be normally dispersive provided LNL << LD. This ensures that significant SPM broadening takes place before the pulses are reduced in intensity due to the normal dispersion. As an example, PCF filled with liquid carbon disulfide [14] not only exhibits large non-linearity ~ $6W^{-1}m^{-1}$ at 775 nm, but can also be tailored to minimize dispersion at the pump wavelength.

REFERENCES

1. J. M. Dudley, G. Genty, and S. Co en, “Super-continuum generation in photonic crystal fiber,” Rev. Mod. Phys. **78**, 1135-1184(2006).
2. A. Rulkov, M. Vyatkin, S. Popov, J. Taylor, and V. Gapontsev, "High brightness picosecond all-fiber generation in 525-1800nm range with picosecond Yb pumping," Opt. Express **13**, 377-381 (2005)
3. T. Schreiber, J. Limpert, H. Zellmer, A. Tunnermann, and K. Hansen, "High average power supercontinuum generation in photonic crystal fibers", Opt. Comm. **228**, 71-78 (2003)
4. J. M. Stone and J. C. Knight, "Visibly “white” light generation in uniform photonic crystal fiber using a microchip laser," Opt. Express **16**, 2670-2675 (2008)
5. A. Kudlinski, A. K. George, J. C. Knight, J. C. Travers, A. B. Rulkov, S. V. Popov, and J. R. Taylor, "Zero-dispersion wavelength decreasing photonic crystal fibers for ultraviolet-extended supercontinuum generation," Opt. Express **14**, 5715-5722 (2006) P. A. Champert, V. Couderc,
6. P. Leproux, S. Février, V. Tombelaine, L. Labonté, P. Roy, C. Froehly, and P. Nérin, "White-light supercontinuum generation in normally dispersive optical fiber using original multi-wavelength pumping system," Opt. Express **12**, 4366-4371 (2004) C. Xiong, A. Witkowska, S. G. Leon-Saval, T. A. Birks, and W. J. Wadsworth,
7. "Enhanced visible continuum generation from a microchip 1064nm laser," Opt. Express **14**, 6188-6193 (2006)
8. W. Wadsworth, N. Joly, J. Knight, T. Birks, F. Biancalana, and P. Russell, "Super-continuum and four-wave mixing with Q-switched pulses in endlessly single-mode photonic crystal fibres," Opt. Express **12**, 299-309 (2004)
9. C. J. S. de Matos, R. E. Kennedy, S. V. Popov, and J. R. Taylor, "20-kW peak power all-fiber 1.57-μm source based on compression in air-core photonic bandgap fiber, its frequency doubling, and broadband generation from 430 to 1450 nm," Opt. Lett. **30**, 436-438 (2005)
10. C. Xia, M. Kumar, O. P. Kulkarni, M. N. Islam, F. L. Terry, Jr., M. J. Freeman, M. Poulain, and G. Mazé, "Mid-infrared supercontinuum generation to 4.5 μm in ZBLAN fluoride fibers by nanosecond diode pumping," Opt. Lett. **31**, 2553-2555 (2006)
11. S. Coen, A. H. L. Chau, R. Leonhardt, J. D. Harvey, J. C. Knight, W. J. Wadsworth, and P. S. J. Russell, "Supercontinuum generation by stimulated Raman scattering and parametric four-wave mixing in photonic crystal fibers," J. Opt. Soc. Am. B **19**, 753-764 (2002)
12. C. Xia, M. Kumar, M.Y. Cheng, O.P. Kulkarni, M.N. Islam, M.N, A. Galvanauskas, F.L. Terry, M.J. Freeman, D.A. Nolan, W.A. Wood, "Supercontinuum Generation in Silica Fibers by Amplified Nanosecond Laser Diode Pulses," IEEE J. Sel. Top. Quantum Electron vol.**13**, no.3, 789-797 (2007)
13. C. Xia, M. Kumar, M. -Y. Cheng, R. S. Hegde, M. N. Islam, A. Galvanauskas, H. G. Winful, F. L. Terry, Jr., M. J. Freeman, M. Poulain, and G. Mazé, "Power scalable